ISSN 0280–5316
ISRN LUTFD2/TFRT--5567--SE

Robustness Analysis of a Wind Power Plant

Egil Overaa

Department of Automatic Control
Lund Institute of Technology
September 1996

Department of Automatic Control
Lund Institute of Technology
Box 118
S-221 00 Lund Sweden

Document name
MASTER THESIS

Date of issue
September 1996

Document Number
ISRN LUTFD2/TFRT--5567--SE

Author(s)
Egil Overaa

Supervisor
Sven Erik Mattson and Anders Rantzer

Sponsoring organisation

Title and subtitle
Robustness Analysis of a Wind Power Plant

Abstract

Stability and performance properties of a wind power plant are analyzed. In particular, the nonlinear effects of time-varying wind are considered. The stability analysis makes use of the Nyquist theorem, the Circle Criterion, and a generalization for periodic perturbations. The robust performance analysis is done by optimization of linear matrix inequalities.

The stability was not found to be a problem, but the specified performance was difficult to prove.

Key words
Uncertain System, Robust Stability, Periodic Uncertainty, Wind Power, and Linear System

Classification system and/or index terms (if any)

Supplementary bibliographical information

ISSN and key title
0280–5316

ISBN

Language
English

Number of pages
42

Recipient's notes

Security classification

Contents

1. Introduction

A wind power plant offers several challenges for control engineers. It should smoothly produce electrical power under large variations in the working environment. The plant should therefore be robust against wind variations and other types of perturbations. One example of such a perturbation is the lee of the tower. Every time, a blade passes behind the tower some aerodynamic torque is lost.

In analysis of control systems the uncertainty of the model is important since the presence of feedback can amplify the sensitivity to perturbations. Controllers that are designed to optimize certain design criteria, may at the same time increase the sensitivity to unmodeled dynamics.

The theory of robust control offers opportunities to address these issues. The purpose of this Master thesis is to demonstrate this on a wind power plant with uncertain parameters and significant non-linearities. It is analyzed in a simple framework combining techniques from absolute stability theory and numerical optimization of linear matrix inequalities.

The analyzed plant and controller design has been successfully operating for several years. The computational analysis of this paper is confirmed on a sophisticated and complex (simulation) model of the real system [Mattsson [6]]. This nonlinear model is much more advanced than the linearized model used for design.

1.1 Organization of the Thesis

In addition to presenting the model, Chapter 2 ties the work of this thesis to the PhD thesis that is model is taken from [Mattson [6]]. It explains in short the complex system of a wind power plant and emphasizes the main points concerning the control design and the control model. Chapter 3 explains some of the methods and criteria used, and also gives some simple examples. This chapter is intended to make the thesis more self-contained and also give some motivation for exploring the effect the perturbation has on the system. It can be omitted or used as a reference when reading the thesis. The main body of the thesis lies in Chapter 4 and 5 where the analysis of the model is conducted. Chapter 4 contains the stability analysis and Chapter 5 the performance analysis. These two chapters are strongly interrelated to each other. The conclusion, summarizes the findings and give a interpretation of its importance.

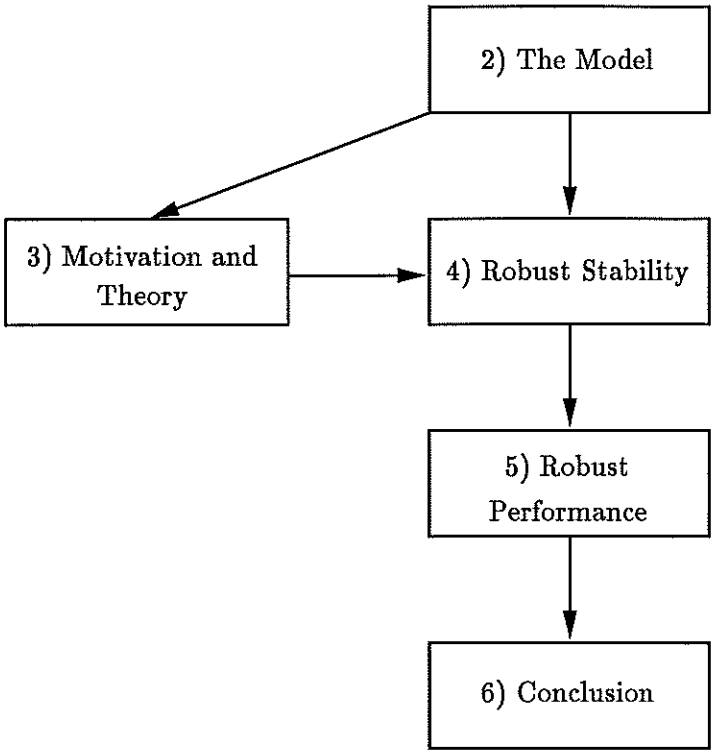

Figure 1.1 The Organization of the thesis

2. The Model

In this chapter we will discuss the dynamics of the wind power plant. The plant studied is a WTS-3 Swedish wind power plant, but the techniques can be extended to other wind power plants or other dynamical systems. This chapter is meant as a background for the rest of the thesis and ties Sven Erik Mattsson's PhD-thesis [[6]] with the work of this thesis.

The model will be divided into three major parts: the turbine, the generator and the wind. In the following the power plant is studied from several viewpoints: a control design model, an analysis model, and a more sophisticated simulation model. First, the design model is presented, and then the simulation model is briefly introduced. The analysis model will be introduced in Chapter 4.

2.1 The Wind Power Plant

The wind turbine is a complex system with three major degrees of freedom. The main movement is of course the rotation of the turbine around its own axis. This movement is enforced by converting the wind energy. There is also a movement of the nacelle and the turbine around the axis of the tower. This movement is called yawing and it concerns the problem of aligning the wind with the axis of the turbine. Yawing is not considered in this thesis. The blades can be turned around their own longitudinal axes, and this is used to control the aerodynamic torque of the turbine.

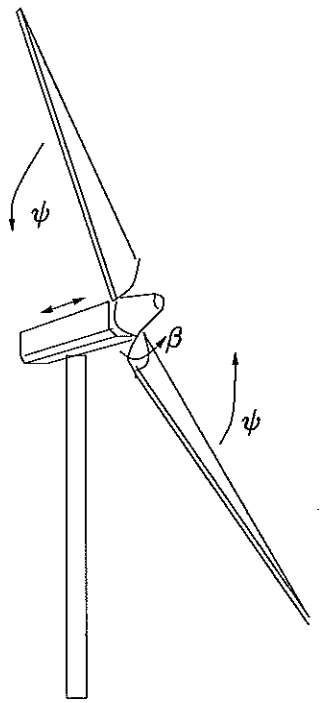

Figure 2.1 The Wind Power Plant

The rotational velocity of the turbine is represented by $\dot{\psi}$. The twist of the

blade around its own axis β is called pitch angle, and it is a variable we can control.

2.2 The Turbine and Generator

In the control design the two most important parts are, not surprisingly, the turbine and the generator. The generator rotates with synchronized speed imposed by the electrical net. The turbine is connected to the generator through a soft shaft, which enables the turbine to oscillate relatively to the generator. This connection will be further studied in the sequel.

The Turbine

The turbine of a large horizontal axis wind power plant is, as expected, big. The length of each of the two blades is 40 m (131 ft) so the turbine covers a rather large disc intersecting the wind.

Notice that the size of the disc is important when designing a control system in the sense that it complicates the design. When designing the control system, it is important to know the average wind speed. It is shown in Mattsson [6] that the wind speed in one point often is poorly correlated (< 0.6) with the mean wind speed over the disc. Consequently, it is not sufficient to measure the wind speed by a wind gauge (anemometer) in one point close to the turbine. However, the wind speed can be estimated using a Kalman filter.

The aerodynamic description of the turbine is rather complicated. The models of trusts and torques are found using static- and two-dimensional airfoil theory to the cross sections of the blades. These equations of torque and trust are used to develop simpler linearized equations:

$$\begin{aligned} \Delta T &= T_\beta \Delta\beta + T_U \Delta U_0 + T_{\dot\psi} \Delta\dot\psi + T_\psi \Delta\psi \\ \Delta F &= F_\beta \Delta\beta + F_U \Delta U_0 + F_{\dot\psi} \Delta\dot\psi + F_\psi \Delta\psi \end{aligned} \tag{2.1}$$

where F is the horizontal force on the turbine, and β is the pitch angle of the blades. This variable is very important since this is a variable we can control. Another very important variable is U_0 — the wind speed. The aerodynamic torque T drives the turbine.

The torque $T(\beta, U, \dot\psi, \psi)$ is very dependent on the wind U and its powers up to the third degree (U^3, U^2 and U). It depends linearly on β and on the second power of $\dot\psi$ ($\dot\psi^2$).

The basic dynamics of importance for pitch angle control is given by the oscillations of the turbine against the electrical grid as depicted in Figure 2.2. This figure should be interpreted as if the electrical network is rotating with constant synchronous speed ($\dot\psi_0$). The "soft shaft" illustrated by the damper and spring transfers the kinetic energy of the turbine to the generator.

The turbine will be said to rotate with an angular velocity $\dot\psi$ of $P = 2.618$ rad/s.

The Drive Train

The important features of the drive train is the step up gearing and the torsional compliance. The gearbox steps up the torsional speed 60 times. The

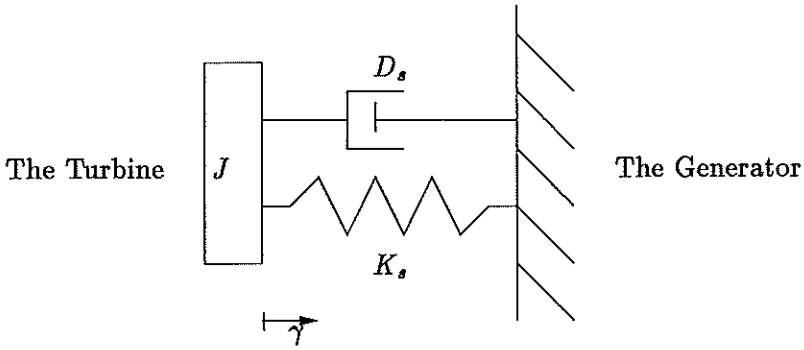

Figure 2.2 The Wind Power Plant

mounting of the planetary gearbox is designed to make the drive train torsionally soft. The equations of the turbine are:

$$\begin{aligned} \Delta T &= J\Delta\ddot{\gamma} + D_s\Delta\dot{\gamma} + K_s\Delta\gamma \\ \Delta\dot{\psi} &= \Delta\dot{\gamma} \end{aligned} \tag{2.2}$$

where J represent the turbine inertia, K_s and D_s are spring- and damping-coefficients (see Figure 2.1).

This simple model contains the first oscillating mode, where the turbine oscillates against the electrical part. The second mode which is the oscillations of the rotor of the generator against the grid can be neglected. The natural frequency of this mode is 25 times higher than the frequency of the first mode and it can neither be excited by the wind variations nor damped by the pitch angle control.

The soft shaft of the power plant is of great importance when studying the system. This flexible design adds a mode with natural frequency 1.2 rad/s (or $0.46P$). This mode is exited by the wind and blade angle changes, but it also works as a low pass filter reducing the effect rapid wind variations have on the electrical output.

The Generator

The power plant generates its electricity through a synchronous generator. The electrical energy (P_E) is given by $\dot{\psi}_0 T_E$ where T_E is the electrical torque. From Figure 2.2 we find that $\Delta T_E = D_s\Delta\dot{\gamma} + K_s\Delta\gamma$ and thus

$$\Delta P_E = \dot{\psi}_0(D_s\Delta\dot{\gamma} + K_s\Delta\gamma) \tag{2.3}$$

where $\dot{\psi}_0$ is the synchronous turbine speed (see Figure 2.1).

The Blade Servo

The dynamics of the blade servo is also important since this will be our only control variable. The turning of the blade around its axis (see Figure 2.1) is described by

$$T_{bs}\dot{\beta} = \beta_r - \beta \tag{2.4}$$

where β_r is the control-input to the servo, and T_{bs} is a time constant (0.4 s). It is also worth noticing that the servo cannot turn the blade faster than 6°/s.

2.3 The Wind

The wind is, obviously, very important for the operation of the wind power plant. It is the energy supply. In the model used for control the wind will be represented by one value for the wind speed. It can be thought of as the mean wind speed. The change in the wind-speed is described by the dynamic by:

$$\Delta\dot{U} = \frac{\Delta U}{T_w} + \sigma_w\sqrt{\frac{2}{T_w}}w \tag{2.5}$$

where w is white noise with zero mean, the time constant $T_w = 20s$ and the standard derivation σ_w is $5-20\%$ of U (the average wind speed over the disc). This dynamic description is important when the controller is designed using LQR algorithms.

Downwind Plant

The power plant studied is a WTS-3 model where the turbine operates downwind of the tower. This means that the turbine alignment (or yaw movement) is supported by the wind, so the alignment can be designed with passive control. In contrast, upwind power plants need active control to align the turbine against the wind. The WTS-3 has an active yaw controller since the passive downwind design was found to be oscillating.

Downwind design has a major drawback to upwind design - the tower blockage. In downwind operation, the plant converts the wind to energy after blowing past the tower that supports the turbine. Upwind power plants on the other hand convert the wind before it reach the tower. The lee from the tower can be modeled as a drop in the torque of each blade when passing behind the shaft. The lee covers a sector modeled as 10° of the rotation of the turbine. Obviously, it occurs twice every rotation of the turbine since this plant has two blades. In other words, it occurs with a frequency of $2P$. The problems connected to the tower-blockage will be studied in this thesis.

In this thesis the change in torque due to the tower blockage is viewed as a change in the velocity of the wind. Instead of saying that the turbine lose the torque on one blade we will just assume that the wind speed is reduced. Thus, the tower blockage is modeled as a periodic disturbance in the wind-speed.

2.4 The State-Space Model

The above equations (2.1 to 2.5) are used to make a linear state-space model around a operating point. This model is used to design a control system for the plant.

$$
\begin{aligned}
\dot{x} &= Ax + B\beta_r + B_U U \\
y &= Cx \\
x &= \begin{bmatrix} \Delta\beta \\ \frac{\Delta U}{100} \\ \Delta\dot{\gamma} \\ \Delta\gamma \end{bmatrix}, \qquad A = \begin{bmatrix} -\frac{1}{T_{bs}} & 0 & 0 & 0 \\ 0 & -\frac{1}{T_{bs}} & 0 & 0 \\ K_\beta & K_U & K_{\dot{\psi}} & K_\psi \\ 0 & 0 & 1 & 0 \end{bmatrix} \\
B &= \begin{bmatrix} \frac{1}{T_{bs}} \\ 0 \\ 0 \\ 0 \end{bmatrix}, \qquad B_U = \begin{bmatrix} 0 \\ \sigma_w\sqrt{\frac{2}{T_w}} \\ 0 \\ 0 \end{bmatrix} \\
y &= \begin{bmatrix} P_E \\ \dot{\psi} \end{bmatrix}, \qquad C = \begin{bmatrix} 0 & 0 & \frac{\dot{\psi}_0 D_S}{10^6} & \frac{\dot{\psi}_0 K_s}{10^6} \\ 0 & 0 & 1 & 0 \end{bmatrix}
\end{aligned}
\tag{2.6}
$$

where we introduce $K_\beta = T_\beta/J$ to simplify notation.

Notice that in the rest of the rapport the Δ's will be dropped to get a cleaner and less confusing representation.

Keep in mind that, the torque $T(\beta, U, \dot{\psi}, \dot{z})$ depends on all the variables β, U, $\dot{\psi}$ and $\dot{z}$. Equation 2.1 is a linearized expression around an operating point. Moreover, constants are used for the variables K_β, K_U, $K_{\dot{\psi}}$ and K_ψ. To linearize equations is always a critical step, and we need to justify that the linearization is valid over the range it covers. This problem will in the following be transformed into a parametric uncertainty problem and studied in detail through Chapters 4 and 5.

2.5 The Simulation Model

For testing the different control proposals derived from the dynamic system described over, the controller was tested on the more complex simulation model [Mattsson [6]]. This model was developed in Simnon and consisted of six different model parts which were connected through their variables. The different parts were: the Turbine, the Synchronous Generator, the Drive Train and Gear-box, the Pitch Servo, the Wind, and the Bus (electrical net). These models do not suffer under the hard assumptions of the linear model described above. Thus, the model gives a much more realistic behavior of the real system. Notice, that the model has been extensively compared with the real wind power plant and confirmed to be good.

3. Motivation and Theory

This chapter contains background material for the analysis given in the thesis. The aim is to establish the notation, to review and summarize the techniques utilized, and to give an engineering motivation. Methods from traditional frequency analysis as well as modern tools for analyzing uncertain systems are described.

3.1 Uncertainty in Models

When modeling a physical system, there is always a mismatch between the model and the real system. This difference is often referred to as a model uncertainty. An engineers goal when modeling a plant is to make a model that gives useful predictions at a low cost. The engineer must, therefore, be a mediator between the physical system and its mathematical model, always keeping in mind the cost of every new detail lumped in to the model.

Feedback systems in themselves are designed for making the plants more robust to uncertainties, but one of the costs for this improvement is the danger of unacceptable behavior and instability. In control engineering the uncertainty of the model should be considered since the concept of feedback can greatly amplify the sensitivity to perturbations.

Methods for analyzing risks for instability are important in control engineering. However, the limitation on the design is more often imposed by poor behavior than loss of stability — i.e. if an electrical circuit is stable for components of 10% accuracy maybe it only behaves well enough when 5% accurate components are used.

Parametric Uncertainty

The mathematical description of a physical object includes several real constants called parameters. Often, the values of these parameters are uncertain or actually varying. The reasons for this kind of uncertainty are often manifold and fall into on or several of the following points:

- The parameter varies from plant to plant. Similar design does not guarantee that the parameters will be the same.
- The parameter is obtained from a linearized expression which may depend on one or many variables.
- Assumed operating condition varies in an unforeseen ways (e.g., stalling at the blades of the power plant)

These factors introduce uncertain parameters to the control design since it is, intentionally, kept simple and, therefor, on a low order with few variables (or states).

When studying the validity of a model, the uncertainty itself needs to be modeled or described in some sense. We want to give a description of the error — the difference between the physical object and its mathematical description.

One way of describing an error due to linearization is to define some bounds on the error. This is done in an effective way by introducing a "conic sector" around the linearization which shows the error.

The most important uncertainty in the model studied is due to linearization of the expression for aerodynamic torque T (2.1). This approximation leaves us with three parametric uncertainties K_β, K_U and $K_{\dot{\psi}}$. A "conic-sector" is shown in Figure 3.1 to illustrate the error of the linearization.

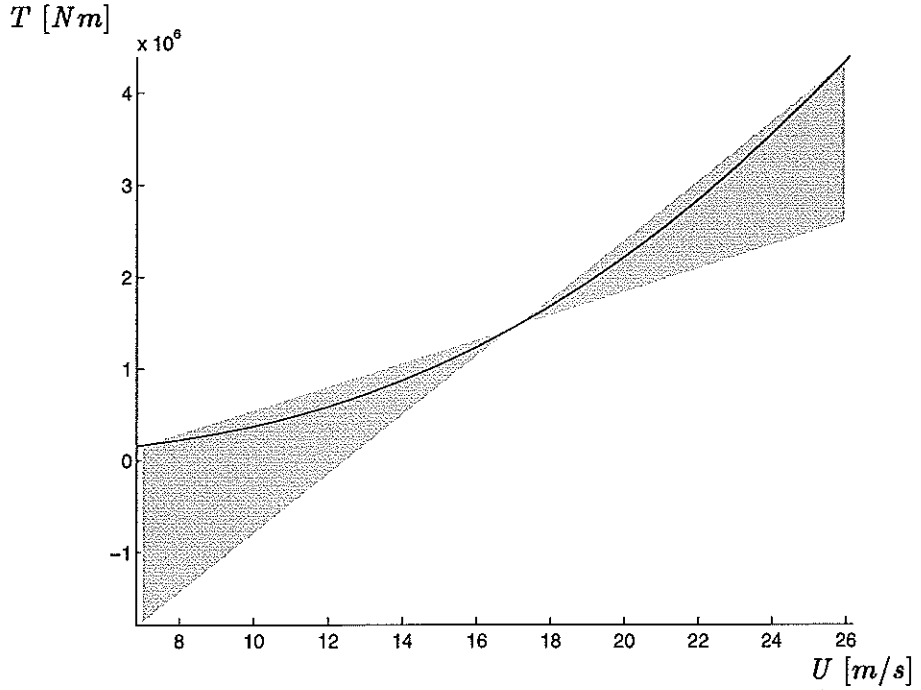

Figure 3.1 Wind speed versus aerodynamic torque T. The parameter β is constant at its opperating point value.

It is also useful to limit the parameters by estimating the upper and lower bound for the real values.

$$\phi \in [\phi_{min}, \phi_{max}] \tag{3.1}$$

This is, for example, done for K_β, K_U and $K_{\dot{\psi}}$ in the following analysis.

3.2 Parametric Perturbations

When analyzing the effect of uncertainties on the stability and behavior of the compensated system, we need to separate the nominal state-space model from the uncertainty. One effective way to do this is to describe the perturbation as a block in the feedback loop.

Robust Stability

To analyze the robust stability of the system, the nominal model is analyzed together with a description of the uncertainty. The model can be represented as a scalar feedback loop (see Figure 3.2).

Transforming the System into a form for Stability Analysis

To analyze the system, we first need to define two new variables: one for variable that is multiplied by the uncertain parameter, and one for the product.

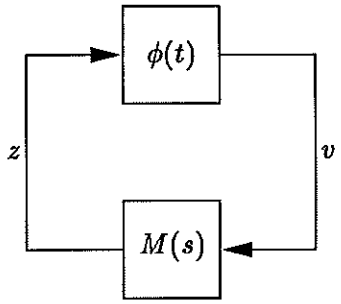

Figure 3.2 Feedback representation of uncertainty

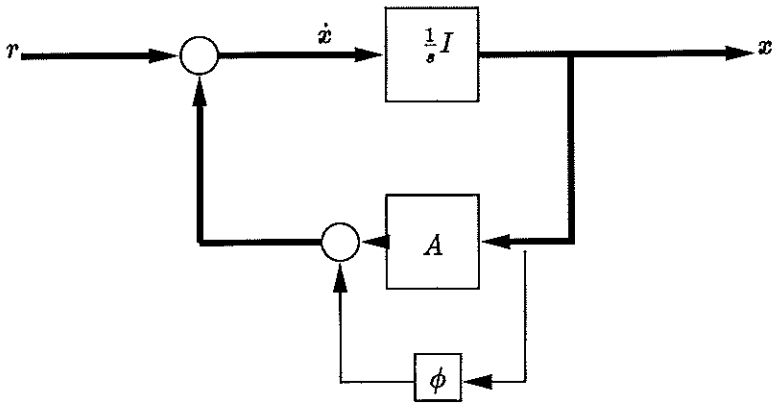

Figure 3.3 Standard State Space Model with Parametric Uncertainty

We then construct a state-space representation of the system with the uncertainty separated from the rest of the equations. For example:

$$\begin{aligned} \dot{x} &= Ax + \alpha_\phi v \\ z &= {\beta_\phi}^T x \\ v &= \phi z \end{aligned} \tag{3.2}$$

from Figure 3.3.

From these equations the block-diagram can be transformed into Figure 3.4 by following the input and output signals.

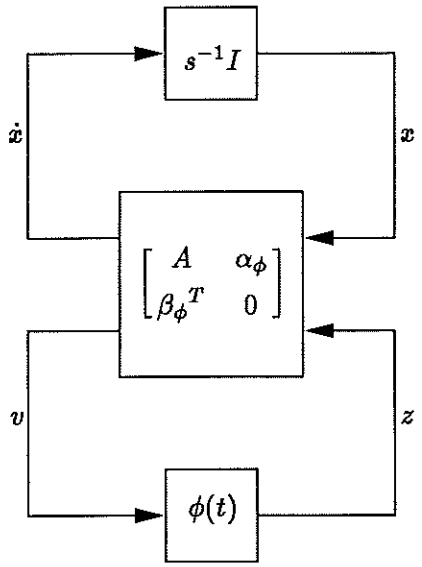

Figure 3.4 More convenient representation of the system

Robust Performance

In most systems, restrictions on the performance limit the design more than the stability. Even though the system is stable, the performance can change much with increasing mismatch of the model and the physical object.

When analyzing robustness performance, the first step is to choose the variables for which the performance is evaluated. For example, we may choose wind-speed and electrical power for the wind power plant. The gain between the two variables is preferably small since ideally the changes in wind speed does not effect the output power.

When the variables are decided, the system is transformed into Figure 5.1. In this form the performance can be analyzed using for example optimization of linear matrix inequalities as will be shown in Chapter 5.

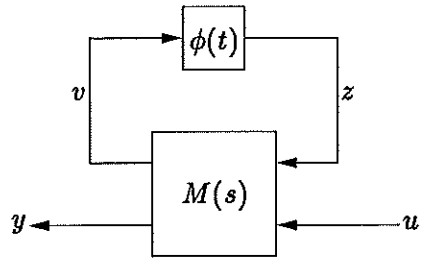

Figure 3.5 Performance analysis setup

3.3 Frequency Domain Analysis

When analyzing stability for parametric perturbations, the frequency domain criteria are used both for the model with a constant and a time-varying uncertainties. A normal procedure for evaluating the stability of the plant with drifting parameters is to start by assuming a simple description of the plant

(i.e. state-feedback) and constant uncertainty; then, move to the more complex plant (i.e. including observer) and time-varying uncertainty. The analysis alternates between increasing the complexity of the model and describing the uncertainty better. The goal is to get a reasonable understanding of robustness properties.

Nominal Plant with Unknown Constant

Consider the case where ϕ is constant but unknown and takes different values in the range of its bounds (see 3.1). This can easily be studied using the Nyquist theorem. From this analysis we get the uncertainty bounds that will give a stable system if the uncertainty is constant (i.e. constant components that are different from plant to plant). If the estimated uncertainty (3.1) is fully covered by the bounds from the analysis, we move on to a more complicated description of the uncertainty.

Nominal Plant with Time-varying Parameters

Analysis of stability for time-varying uncertainly is often referred to as "absolute stability analysis". The main tool in this analysis is the Small Gain theorem and its graphical counterpart the Circle Criterion. The Circular criteria will be reviewed here.

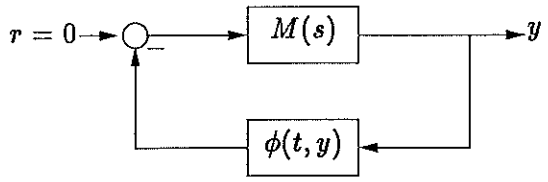

Figure 3.6 Model configuration for the Circle Criterion

THEOREM 3.1—CIRCLE CRITERION
Assume that ψ is Lipchitz. Then

$$\dot{x} = Ax - B\phi(t, Cx), \quad x(0) = x_0 \tag{3.3}$$

is asymptotically stable if there is a α, β (with $\beta > \alpha$) such that:

$$\alpha y \leq \phi(t, y) \leq \beta y \quad \forall t, y \tag{3.4}$$

and

$$Re\left[\frac{1 + \beta M(j\omega)}{1 + \alpha M(j\omega)}\right] > 0 \quad \forall \omega \in R \tag{3.5}$$

□

The name of the theorem refers to the geometrical interpretation of the theorem where the sector of the non-linearity is presented as a circle passing through the point $-\frac{1}{\alpha}$ and $-\frac{1}{\beta}$ [Khalil [4]].

Instead of using the Circle criterion directly, we sometimes plot the invert Nyquist contour. From this curve the interval of stability can be seen directly. There is no need to inverse the values of the crossing-points. As an example, the two different presentations are shown. In this case the stability sector is $\phi \in [-0.67, 0.67]$.

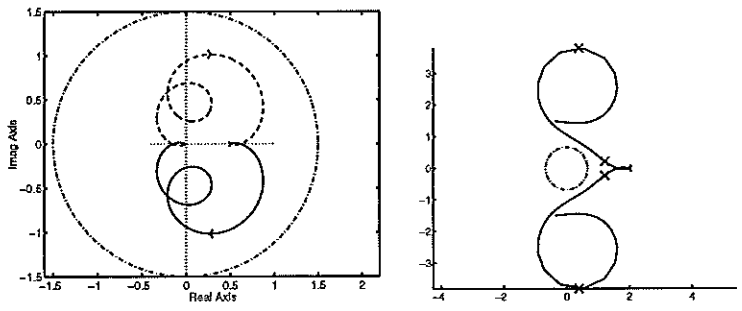

Figure 3.7 Circle criterion and its inverse representation

Willems Periodic Uncertainty Theorem

If the uncertainty is periodic it can be studied more carefully by adding the information of periodicity to the analysis. This enable us to give a more accurate prediction of the system, thus less conservative bounds.

An extended stability theorem for systems with periodic coefficients, as stated by Willems [[10]] is used to examine periodic uncertainties (i.e. tower blockage).

Consider the a system loop as shown in Figure 3.8 where:

1. $M(s) = p(s)/q(s)$, where $p(s)$ and $q(s)$ are real polynomials in s, i.e.,

$$\begin{aligned} p(s) &= s^n + p_{n-1} + \cdots + p_0 \\ q(s) &= q_n s^n + q_{n-1} + \cdots + q_0 \end{aligned}$$

   with p_i and q_i real numbers.

2. $\phi(t)$ is real valued piecewise continuous periodic function with period T
3. Either $q_n = 0$, or $-1/q_n \in [\alpha, \beta]$ is satisfied.

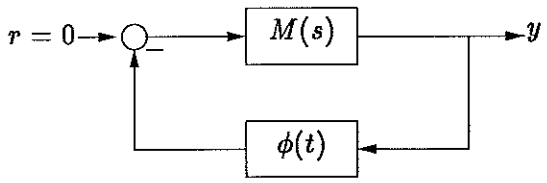

Figure 3.8 Feedback System

The frequency domain theorem of Willems can then be stated as:

THEOREM 3.2
The system is asymptotically stable if

1. $p(s) + \phi q(s)$ has all its zeros in $Re(s) < 0$ for some $\phi \in [\alpha, \beta]$,
2. there exist a real function of s, $F(s)$ such that for all real ω
   (a) $ReF(j\omega) \geq 0$,
   (b) $F(j(\omega + \omega_0)) = F(j\omega)$ where $\omega_0 = \frac{2\pi}{T}$,
   (c) $Re\left\{F(j\omega)\frac{1+\beta M(s)}{1+\alpha M(s)}\right\} > 0$.

□

3.4 Conclusion

In this chapter we have outlined the technique to be used for analyzing the uncertain system. The procedure can be summarized as:

- Represent uncertainty by a feedback loop.
- Analyze the stability of the loop with the uncertain element.
- Analyze the performance of the system taking count of the uncertain element.

Through the rest of the thesis the method outlined will be used to analyze the effect the major parametric perturbations will have on the stability and behavior of the wind power plant.

4. Robust Stability

In this chapter the control of the Wind Power Plant proposed by Mattson [6] will be analyzed through its parametric uncertainties. The design procedure of the control system exploit simple linear time invariant state space models. The model where given by the linearized physical equation (2.6).

This linear model simplified the design procedure, but raised the question if the control law guaranteed the stability.

In 1984 when the control design was done, Simulations were used to evaluate performance and robustness. Amplitude and phase margins were also used to measure robustness. Unfortunately, requirements on performance and robustness are indeed conflicting. It makes the trade off between performance and robustness a key issue. This makes methods to analyze effects of uncertainties and nonlinearities very interesting in this application.

In the following, the robustness of the systems stability will be analyzed when the plant is affected by uncertainties. Thus, an evaluation of the systems stability can be developed for the uncertainties that influences the system.

4.1 The Major Uncertainty in the Model

The dynamical equations are used to construct a linear model around and operating point of U=18m/s. The power plant is running for winds in the range of 7m/s to 27m/s which stretches the reliability of the linearized model very far, since both K_β, $K_{\dot{\psi}}$ and K_U are very dependent on the wind speed. It will be seen in the following that the uncertainty in K_U is of no importance when we consider the stability of the model.

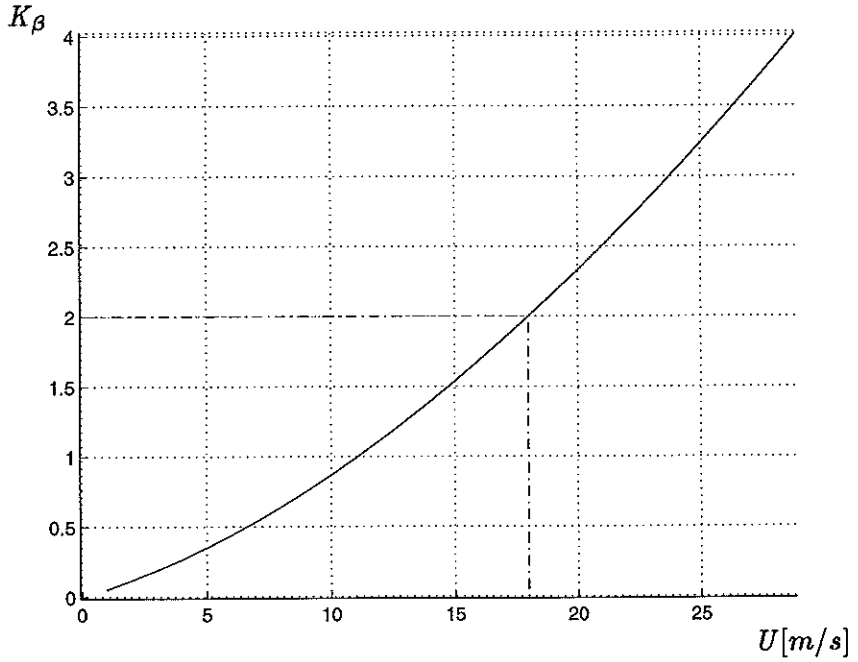

Figure 4.1 Wind speed versus K_β

K_β, on the other hand, has a great impact on the stability and will be studied in detail throughout this chapter. A system where both K_β and $K_{\dot{\psi}}$

are examined at the same time will also be studied in the sequel. K_β is found from the rather complex wind model, and by assuming that the change in the wind speed after blowing through the turbine is not dependent on the pitch angle the function can be written:

$$K_\beta = \frac{R^3 cos^3(\varphi)\dot{\psi}^2}{J_t}\left(A_2\frac{(1-a)U}{R\dot{\psi}} + \frac{1}{2}A_0\left(\frac{(1-a)U}{R\dot{\psi}}\right)^3\right) \tag{4.1}$$

Most of the parameters in this function are either constants or assumed to be constant. The parameter R is the length of the blades, J_t is the inertia of the turbine, φ is the flapping angle of the blades (assumed constant), the A's are aerodynamic constants of the blade and $\dot{\psi}$ (the angular velocity of the blades) is assumed to be constant.

The variable (K_β) does not dependent on β, but, is non-linear in U. The variable K_β can be seen as a time varying uncertain parameter (see Figure 4.1). The gain range used in the sequel is $K_\beta \in (0, 4)$ which is the interval found in [Mattsson [6]].

4.2 The State Feedback Model

The variable K_U is has no effect on the stability. This can be seen since this variable is not in the feedback loop (see Equation 2.6). Thus, K_U will not influence the stability. The wind is just an input to the whole system, and the uncertainty of K_U can be seen together with the uncertainty of U itself. K_β, on the other hand, is in the loop and we will study this parametric uncertainty in more depth below.

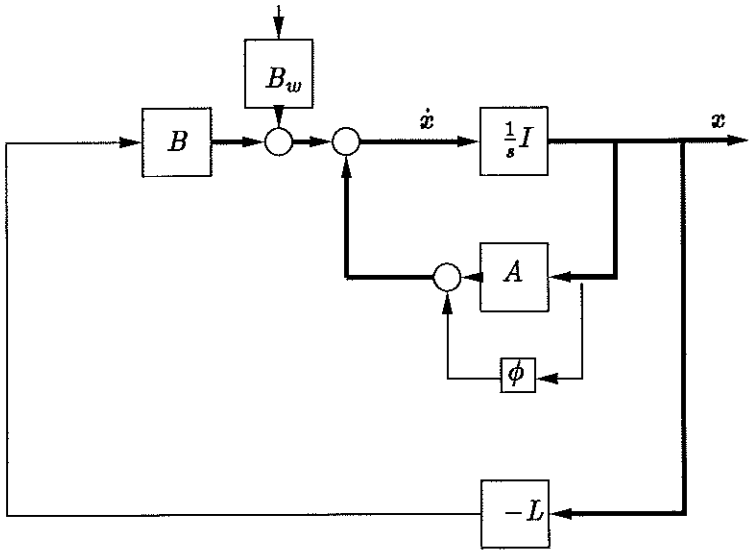

Figure 4.2 State feedback control

The uncertain parameter K_β can then be drawn in to the state space model as a time varying parameter ϕ (see Figure 4.2).

The next step is to "move out" the uncertain parameter. This is done by first presenting K_β as:

$$K_\beta = \overline{K}_\beta + \phi(t) \tag{4.2}$$

where $\overline{K_\beta}$ is the operating point value of K_β and $\phi(t)$ is the time varying uncertainty. Thus $\phi(t)$ defines the sector $\phi \in [-2, 2]$. The operating point $\overline{K_\beta} = 2$.

Then the model can be written on the form:

$$\begin{aligned} A &= \overline{A}(t) + \alpha_\phi \phi(t) {\beta_\phi}^T \\ &= \begin{bmatrix} -\frac{1}{T_{bs}} & 0 & 0 & 0 \\ 0 & -\frac{1}{T_{bs}} & 0 & 0 \\ \overline{K}_\beta & \overline{K}_U & \overline{K}_{\dot{\psi}} & \overline{K}_\psi \\ 0 & 0 & 1 & 0 \end{bmatrix} + \begin{bmatrix} 0 \\ 0 \\ 1 \\ 0 \end{bmatrix} \phi(t) \begin{bmatrix} 1 & 0 & 0 & 0 \end{bmatrix} \end{aligned} \tag{4.3}$$

where the respective $\overline{K}$'s correspond to the operating point values of the parameters in Equation (2.6).

The system can then be shown in a new representation:

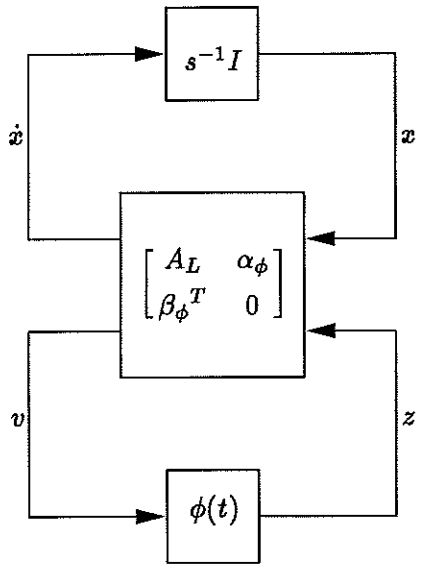

Figure 4.3 Reduced Framework for Robust Stability Analysis

where A_L is equal to $\overline{A} - BL$.

Manipulating the system to move the integrators into the block as Figure 3.2. Notice; since we only are interested in the stability of the loop with the uncertainty, we use a simple scalar feedback loop.

$$M(s) = {\beta_\phi}^T (Is - \widetilde{A})^{-1} \alpha_\phi \tag{4.4}$$

In this representation can the stability analysis can be carried out in an efficient way using some of the powerful frequency domain criteria for instance Nyquist and Circle criterion described in Chapter 3.

Frequency Domain Analysis

The stability of the system is studied; first, optimistically assuming ϕ to be constant, and then in a very pessimistic perspective viewing $\phi(t)$ as the set of all different time varying functions within the sector.

The Nyquist method shows stability in the time invariant case. The interval for which the gain K_β stabilizes the system in a time invariant sense was directly obtained from the inverse of the inverse Nyquist curve (see Figure 4.4). The point k defines the lower bound, and the upper bound is found to be infinite. The stability gains then becomes the set $K_\beta \in [-1.12, \infty)$ which encloses the whole range of wind speeds the plant is designed for (see Figure 4.1).

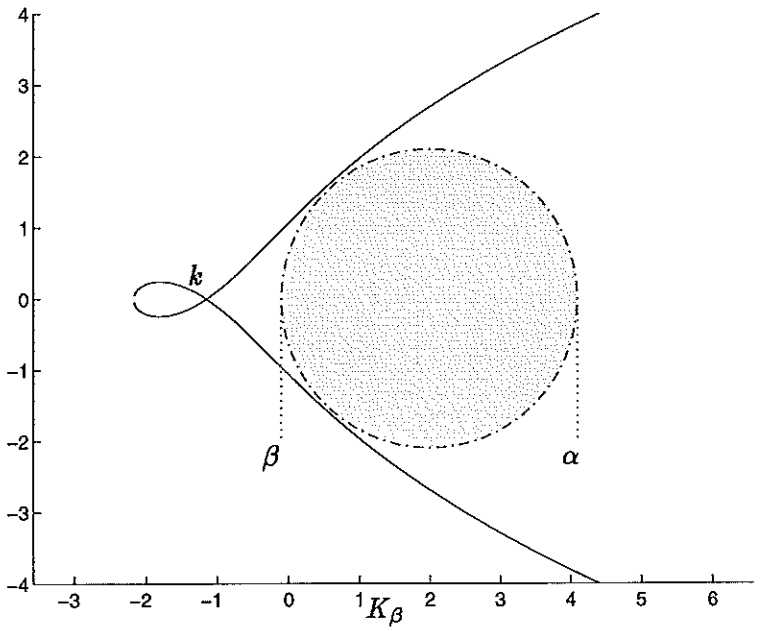

Figure 4.4 Inverse Circle Criterion for state feedback

Using the Circle Criterion we get an absolute stability sector or the sector where K_β can vary freely without the risk of instability. This interval is given by the points α and β to be $K_\beta \in [-0.1, 4.1]$. Thus the stability is guaranteed for this simplified model for time varying uncertainty in the wind in the range of 7m/s to 27m/s (the specified operating range of the wind power plant).

This gives us some confidence, but the real system is more complicated, and to reflect more of the reality a new model is studied.

4.3 Observer Based Feedback

For the observer based model we do not have direct access to the states, but measure the change in the power generated (P_E) and the change in the angular velocity of the hub ($\dot{\psi}$). To estimate the state a Kalman filter was designed and implemented as an observer. The design of the filter was done by linear quadratic Gaussian design, and could be done separately from the feedback design due to the separation principle. The new model was also reduced to a three state system by viewing β as an input, thus eliminating one of the

states. The system then had a form like this:

$$\begin{aligned} \dot{x} &= Ax + B\beta, \quad y = Cx, \\ x &= \begin{bmatrix} \frac{U}{100} \\ \dot{\gamma} \\ \gamma \end{bmatrix} \quad A = \begin{bmatrix} -\frac{1}{T_w} & 0 & 0 \\ K_u & K_{\dot{\gamma}} & K_\gamma \\ 0 & 1 & 0 \end{bmatrix} \\ B &= \begin{bmatrix} 0 \\ K_\beta \\ 0 \end{bmatrix} \quad C = \begin{bmatrix} 0 & \frac{\dot{\psi}_0 D_S}{10^6} & \frac{\dot{\psi}_0 K_s}{10^6} \\ 0 & 1 & 0 \end{bmatrix} \end{aligned} \tag{4.5}$$

and with the observer it could be drawn as in Figure 4.5

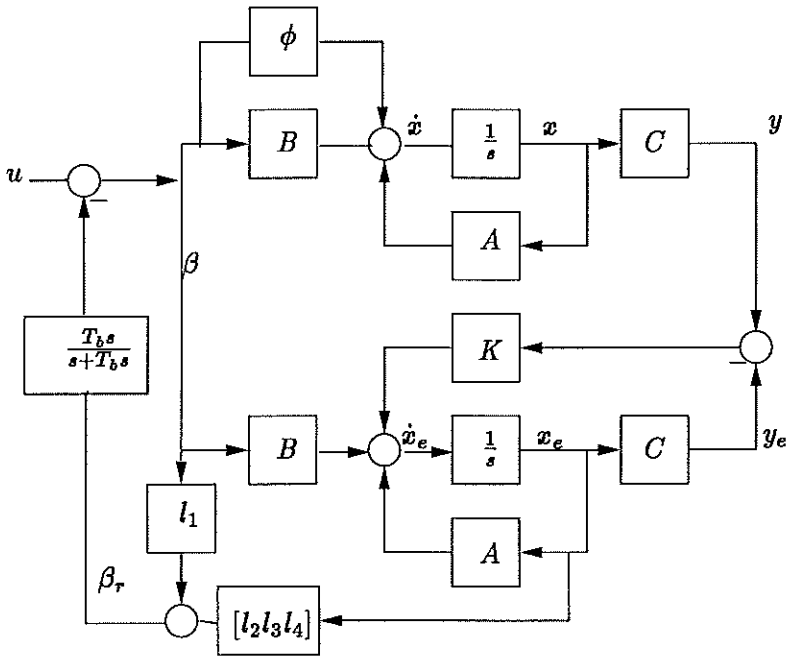

Figure 4.5 State Space model of system with observer and feed back

Notice that the feedback is feed through a filter (the servo of the blade turn) as a part of the model reduction. As seen in the figure, the complexity of the model with the observer is much higher than the one for the first simple model. Thus, transforming the system into a single scalar loop is a bit more complicated.

Stability Analysis

The stability analysis starts by transforming the system into a single feedback loop (3.2) where the uncertainty of ϕ was separated from the rest of the transfer function. The transfer function can be found in an efficient way by writing the system as a compact state space model.

$$\begin{aligned} \dot{x} &= Ax + r \\ \dot{x_e} &= Ax_e + B\beta + K(Cx - Cx_e) \\ \beta_r &= -l_1\beta - [\, l_2 \quad l_3 \quad l_4 \,]\, x_e \\ \dot{\beta} &= -T_{bs}\beta + T_{bs}\beta_r \end{aligned} \tag{4.6}$$

Notice that the uncertainty now is placed in the only element of the B vector for the plant and not in the A matrix as before. In this model B was written as:

$$B = (\overline{K_\beta} + \phi(t)) \begin{bmatrix} 0 \\ 1 \\ 0 \end{bmatrix} \tag{4.7}$$

In this form the Nyquist theorem together with the Circular criterion were utilized to formulate a robustness evaluation.

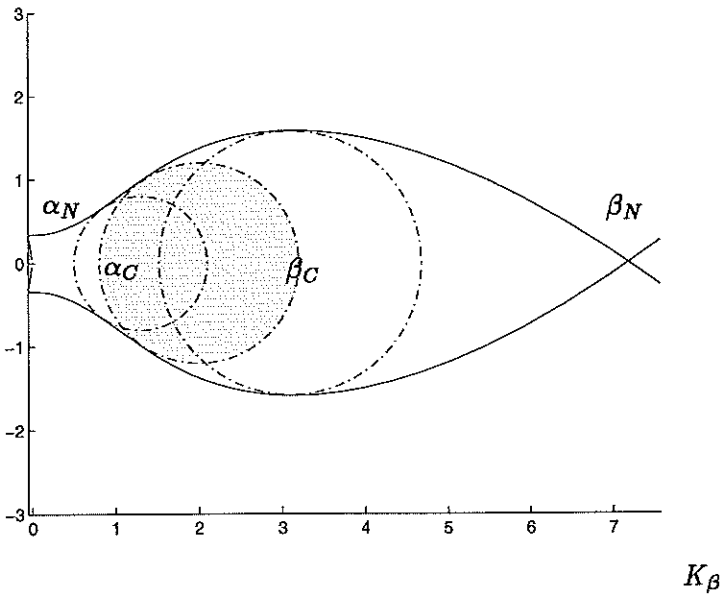

Figure 4.6 Inverse Circle Criterion for observer feedback

First, we study the inverse Nyquist contour of Figure 4.6 to state the region of the stability of the plant when ϕ is constant. The points β_N and α_N define the stable interval with respect to K_β to be $K_\beta \in [0, 7.26]$ (see Figure 4.6). This means that the plant is stable for constant winds in the whole range of K_β and also for wind speeds a lot faster than 27m/s (which is the maximum wind the plant is designed for — see Figure 4.1).

When we look at the stability for the time varying function, on the other hand, the sector does not give a overwhelmingly positive result. The interval corresponding to the points between β_C and α_C is only $K_\beta \in [0.8, 3.2]$ (see Figure 4.6) and that does not cover the wind speeds the plant are designed for.

4.4 Analyzing the System when two Correlated Parameters are Uncertain

As mentioned, the uncertainty in K_β is of most importance for the stability, but also the parameter $K_{\dot{\psi}}$ (the friction) varies with the wind. The two functions $K_\beta(U, \beta)$ and $K_{\dot{\psi}}(U, \dot{\psi})$ were found to have very similar dependency on

the wind speed, and they were therefore lumped into one uncertainty sector with different scaling. By keeping this single input single output structure the system can be analyzed with graphical techniques which are less complicated than general multiple input multiple output analysis. To study this system where two parameters varies in a correlated fashion, the A matrix was written as Equation 4.8.

$$\begin{aligned} A &= \overline{A} + \alpha_\phi(t)\phi\beta_\phi{}^T \\ &= \begin{bmatrix} -\frac{1}{T_{bs}} & 0 & 0 & 0 \\ 0 & -\frac{1}{T_{bs}} & 0 & 0 \\ \overline{K}_\beta & \overline{K}_U & \overline{K}_{\dot{\psi}} & \overline{K}_\psi \\ 0 & 0 & 1 & 0 \end{bmatrix} + \begin{bmatrix} 0 \\ 0 \\ 1 \\ 0 \end{bmatrix} \phi(t) \begin{bmatrix} 1 & 0 & -0.33 & 0 \end{bmatrix} \end{aligned} \tag{4.8}$$

The system can now be studied through the same techniques as before.

Stability Analysis

The inverse Nyquist curve is plotted for this system. Not surprisingly, this system gave different results than the earlier and simpler models. For this system the time invariant stability was found to be $K_\beta \in [0, \infty)$ while the interval for the time varying case the new model was a bit more restrictive than before and gave an interval $K_\beta \in [0.91, 3.09]$.

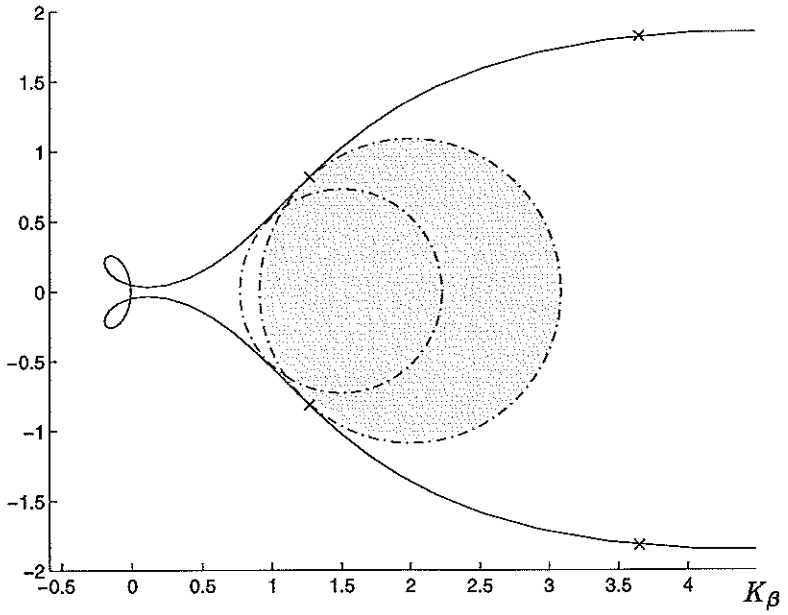

Figure 4.7 Inverse Circle Criterion used for stability analysis of uncertainty

The reason why the time invariant system becomes more relaxed can be that this "new" uncertainty, which can be interpreted as a friction-coefficient, has a opposite effect to K_β and since they both behave similarly with respect to the wind they might cancel out each other in some sense. Notice that both uncertainties are modeled with the same sector only scaled differently (see Equation 4.8).

Results of our Analysis

Through this chapter we have carried out two parallel approaches to the stability analysis: one for the time invariant case and one for the time varying case. In the time varying case the gain $K_\beta(t)$ could vary freely within the sector (see Figure 4.1). These two approaches are both strongly simplified, and our sector model for the uncertainty is very conservative.

To get a better picture of the system more sophisticated models of the uncertainty will be needed. By providing information about the frequency spectrum of the wind speed through the turbine in more detail more advanced techniques can be utilized.

4.5 Periodic Uncertainty

When dealing with periodic systems, there is a great chance that the uncertainty also is periodic. When analyzing a periodic uncertainty, the periodicity gives new and important information. Thus, more advanced frequency domain stability criteria can be utilized. These criteria take advantage of the periodicity as well as the sector limits of the uncertainty.

Tower Blockage

When the turbine spins around its own axis with a constant angular-velocity ($P = \dot{\psi}_0 = 2.618$ rad/s), the blades align with the tower with a frequency of $2P$. This power plant operates in downwind and the tower, therefore, blocks for the wind and steals the aerodynamic torque from the blade. Moreover, the parameter concerning K_β varies a great deal from its assumed constant value in the design-model of the system (see Equation 4.1). This effect is modeled as a square wave. The blade is in the lee for about 10° every time a blade swings behind the shaft. Thus, the aerodynamic torque-drop can be modeled by decreasing K_β to the half for a short while twice every rotation of the wind turbine (see Figure 4.8).

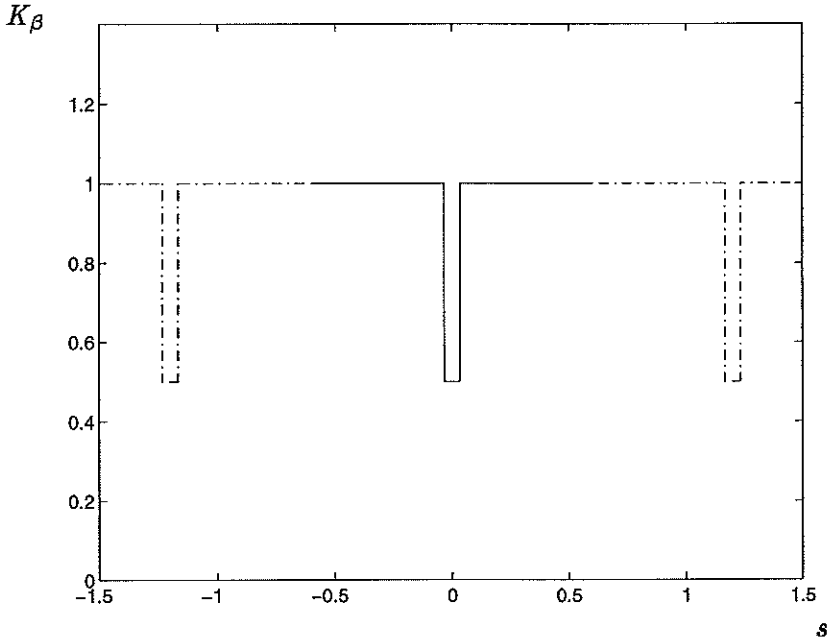

Figure 4.8 A Square Wave Model of the Tower Blockage.

Analysis of the Tower Blockage

By assuming that the wind velocity is constant and the only uncertainty in the system is the tower blockage; the uncertainty can be analyzed in the same way as before in the frequency domain. In this analysis the circles are drawn for a torque reduction to the half of its nominal value (see Figure 4.8 and Figure 4.9). Moreover, the case studied considered losing the torque from one of the blades at the time when the plant is operating under different but constant winds.

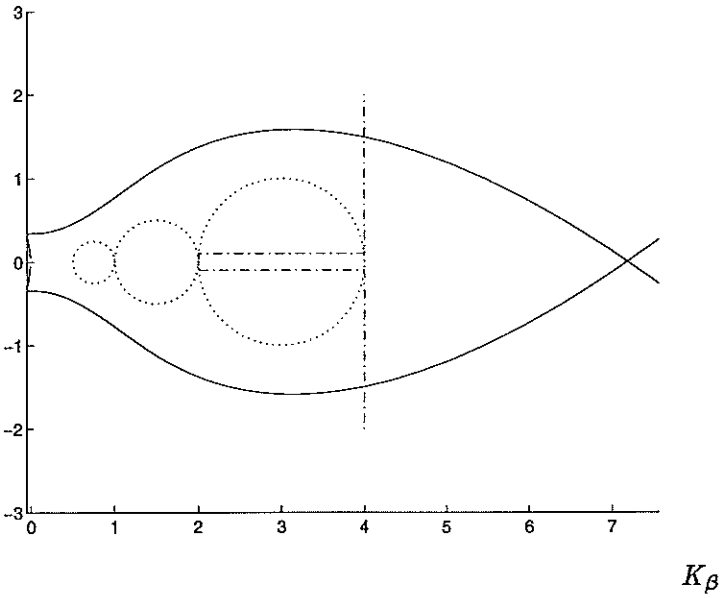

Figure 4.9 Inverse Circle Criterion with Circles Corresponding to Tower Blockage

From the inverse circle criterion plot of Figure 4.9 the stability of the system is guaranteed for changes due to tower blockage when the wind itself is kept constant. Notice how the change in the torque (K_β) due to the tower increases linearly with increasing nominal value for K_β (the circle radius increases). Each circle represents a system with constant wind corresponding to the K_β value of the right edge of the circle and the left edge corresponding to the torque of the turbine when one blade is under the lee of the tower as illustrated in the largest circle.

The stability of the system with respect to the tower blockage was also confirmed by simulations on the more sophisticate model developed in Simnon. This model was tested for different nominal values for the wind speed and with various models for tower blockage, but the tower blockage was not found to be a problem for the stability of the loop.

Frequency Analysis of the System with Two Uncertain Parameters

The new inverse Nyquist curve looks like Figure 4.10, and by drawing the same circles as over (for the tower blockage) we see that the Circle Criterion leaves us inconclusive for small values of K_β — the circle with nominal condition $K_\beta = 0.5$ crosses the Nyquist curve.

By applying an extended stability theorem for systems with periodic coefficients, as stated by Willems [[10]] (see Theorem 3.2), the stability can be shown for this more conservative system.

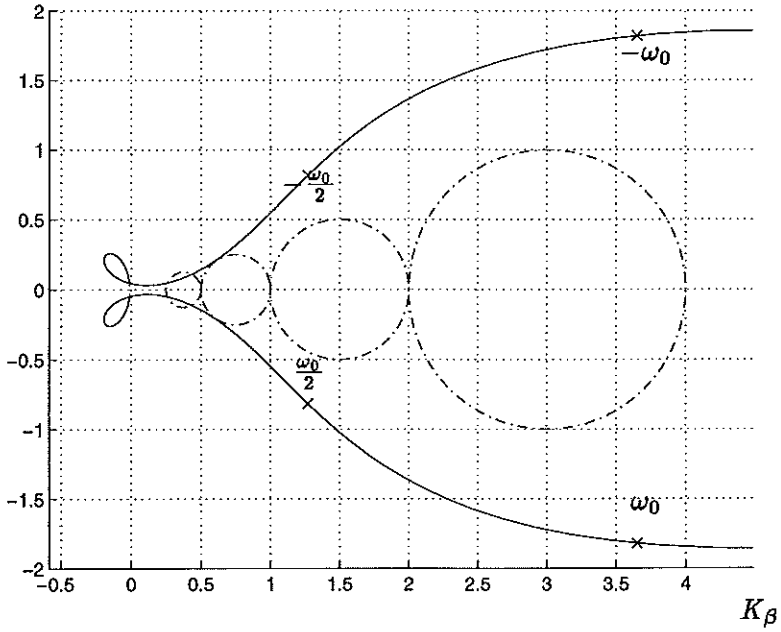

Figure 4.10 Inverse Circle Criterion with Circles Corresponding to Periodic Uncertainty

From Figure 4.11 the shaded circle then illustrates how stability can be proven by the simple and sufficient condition for Willems's stability theorem (see Corollary 4.1)

COROLLARY 4.1—WILLEMS'S THEOREM
The system described in Theorem 3.2 is asymptotically stable if:

1. the Inverse Nyquist locus of $M(s)$ encircles the point α on the negative real axis (notice that the axis in my plot is scaled to correspond with K_β see Equation 4.2) of the Nyquist plane ρ times where ρ is the number of open-loop poles of $M(s)$ in $Re(s) > 0$,
2. there exist a circle C through the points α and β, such that the Nyquist locus of $M(s)$ for $\omega \geq 0$ does not intersect it,
3. C does not enclose any multiple of the periodic frequency ω_0 of $\phi(t)$ for $\omega \leq 0$.

□

From Figure 4.11, the stability of the system for tower blockage can be shown for small values of K_β by constructing similar smaller circles to C.

Some interesting remarks can be added to the conclusion from this theorem. First, the frequency of the periodic uncertainty is of great importance. This can be illustrated by examining the system operating at the constant wind at the operating point ($K_\beta = 2$). Let the uncertainty be assumed to swing the same amount up and down, thus, centering the circle at $K_\beta = 2$. We then see that for $\omega_0 = 2P$ the circle can be made very large (see Figure 4.12) but for lower frequencies the uncertainty sector (or circle) decreases.

Thus by restricting the uncertainty to be periodic the uncertainty sector can be increased with increasing frequency of the periodicity (see figure 4.12).

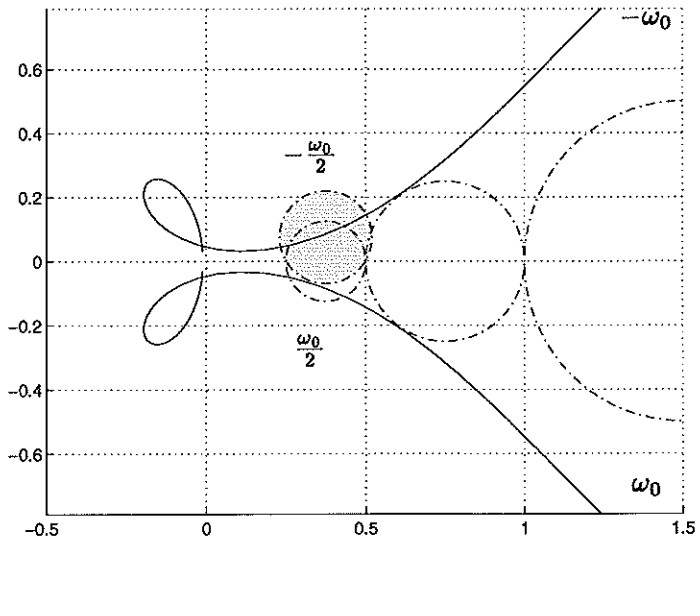

Figure 4.11 Inverse Nyquist Plot and Frequency Analysis of Periodic Uncertainty

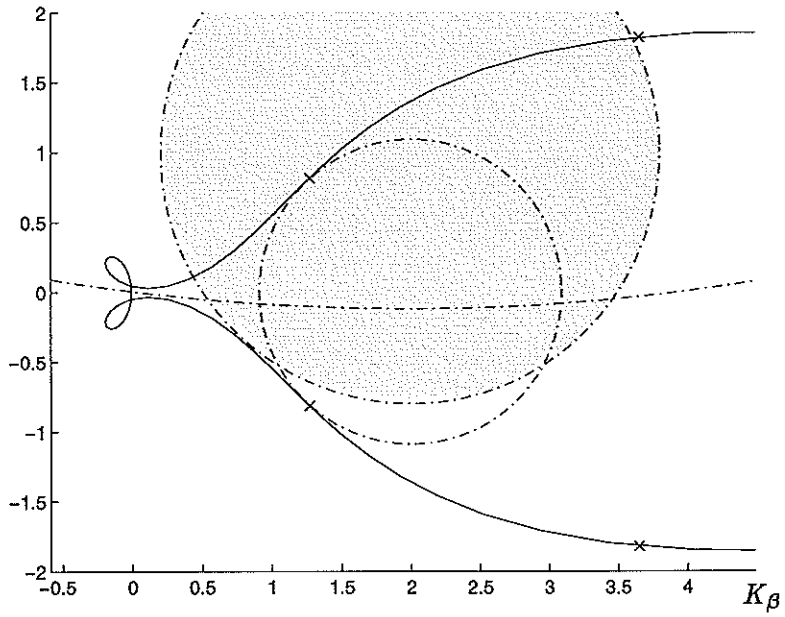

Figure 4.12 Inverse Nyquist Plot and Frequency Analysis of Periodic Uncertainty

4.6 Conclusion of the Robust Stability Analysis

When analyzing the stability of the model, the physical system is approached from two different sides. First, a simple model is made to describe the system and the uncertainty is assumed to be non existing. Then, from the other side, the uncertainty is described by a sector and the system is kept the same. This process is then repeated by, first, making the model more complicated, and in turn describing the uncertainty more precisely.

Through this form of analysis we also need to keep in mind the cause of the uncertainty to be able to give a conservative but realistic description of

the perturbation.

When deriving conclusions from the models a great deal of engineering judgment is needed. On example of this is the study of stability for small K_β. When comparing the values of $K_\beta = 0.5$ with the corresponding wind speed (Figure 4.1), we see that this corresponds to wind speeds in the range of $< 7m/s$. The stability in this region is not very critical since this is barely enough to make the turbine rotate (recall that the operating wind is 7-27m/s).

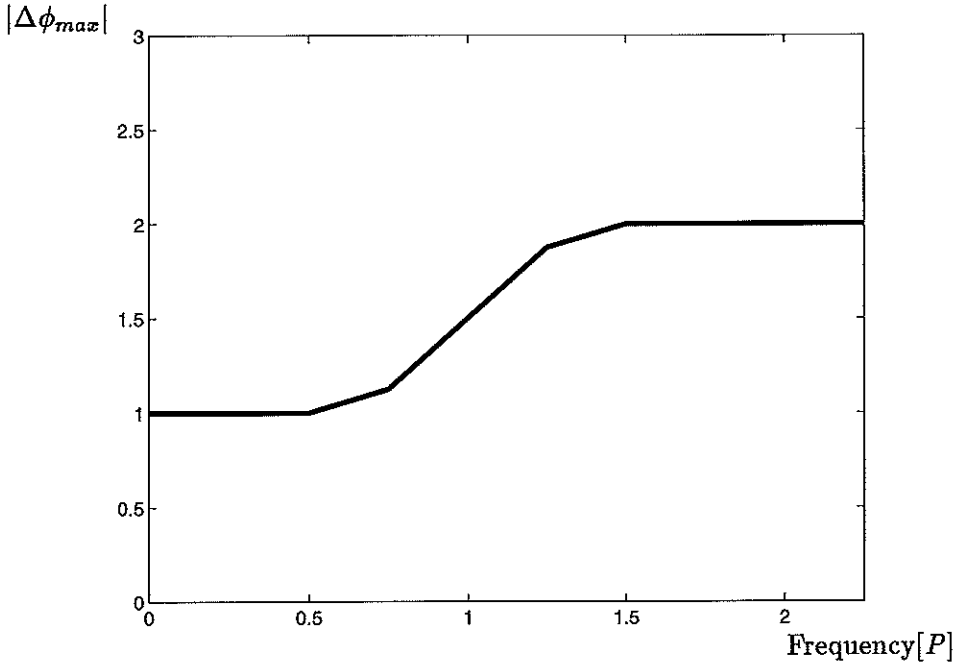

Figure 4.13 Inverse Nyquist Plot and Frequency Analysis of Periodic Uncertainty

In this chapter much work has been devoted to periodic uncertainties. In Figure 4.13 we see how these uncertainties can be allowed to vary more when their frequency increases. This is, in my opinion, rather interesting. Since the system itself behaves in a periodic fashion many of the uncertainties will also behave periodically (i.e. tower blockage).

Notice that uncertainties in the torque with a frequency twice the frequency of the turbine rotation (which is the case for the tower blockage) is not very critical for the system stability. It is also interesting to notice that $\omega_0 = P$ (the frequency of the turbine) only leaves room for a small circle, and the worst range of frequencies is $\omega_0 \in [0, P]$ (see Figure 4.12 and compare with Corollary 4.1).

This analysis is interesting and positive for the stability of the Wind Power Plant since there is no indication in the simulations of the plant that there are any elements that will introduce uncertainty in this range. It would be even more positive if $\omega_0 = P$ not was in the range of low tolerance since it is natural that many of the perturbations will occur with the same frequency as the turbine (e.g., imbalance in the blade weight of the blades, uncertainties of the gears due to wear).

5. Robust Performance

Even though stability of the closed-loop system is considered the first and most important property in robust analysis, robust performance is often of major significance. Changes in the environment of the system (e.g., wind gusts), which result in tracking errors and poor control of the system, often restricts the design. These tracking problems can be greatly amplified by perturbations (e.g., parametric uncertainties) in the system. In many systems, unacceptable performance restricts the magnitude of the upper and lower limits of the parametric uncertainty more than the loss of stability. Thus, the allowance of parametric variation is not determined by the loss of stability but by unacceptable performance. For this reason techniques for analyzing robust performance is very important. Given a limited freedom of parametric change the performance is evaluated through modern techniques involving traditional frequency analysis as well as modern optimization of linear matrix inequalities.

5.1 The Servo Limitations

When designing the control of the Wind Power plant (as well as constructing the whole plant) one of the main goals is to keep the maintenance cost as low as possible. The LQG design, therefore, penalize the servo speed $\dot{\beta}$ in the cost function to restrict the movement of the servo.

To analyze this robustness performance the system is transformed into the standard form of Figure 5.1 [Zhou [11]]. The time-varying uncertain parameters are "moved out" of the nominal-model. Further, the input output variable are corresponding to the performance evaluated.

In this case the wind change (U) is paired with the change in pitch movement ($\dot{\beta}$). The analysis, therefore, gives a measure of how fast pitch-movement is needed for changes in the wind when considering some parametric uncertainty.

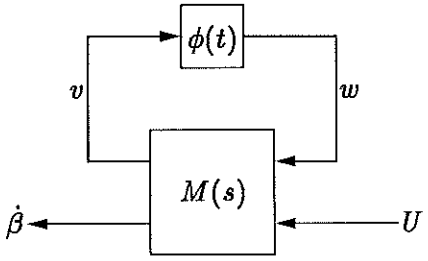

Figure 5.1 General Framework for stability analysis

Recall, from the state-space model that the dynamics of U was given some low pass behavior. Thus, the LQG design gives less wait on high frequency wind. The cost function was then given by:

$$J = E\left\{\lim_{T\to\infty}\frac{1}{T}\int_0^T q^2 P_E^2 + q_\beta^2(\beta_r - \beta)^2 dt\right\} \tag{5.1}$$

where $q = 1$ and $q_\beta = 10$ [Mattsson [6]].

To get the system on the form as shown in Figure 5.1 the dynamics of the wind was removed from the model and U was changed to be an input instead. Moreover, the wind-speed state was deleted from the model — reducing the model to three states. The observer was, as expected, left unchanged (see Figure 5.2. Thus, the system is presenting a equivalent form of Figure 5.1.

Notice that the subscript s indicates the changed model to the three state system. Recall from Chapter 2 that:

$$\dot{\beta} = \frac{\beta_r - \beta}{T_{bs}}. \tag{5.2}$$

This enable us to output $\dot{\beta}$ from this model. Thus the performance from U to $\dot{\beta}$ can be studied from this model.

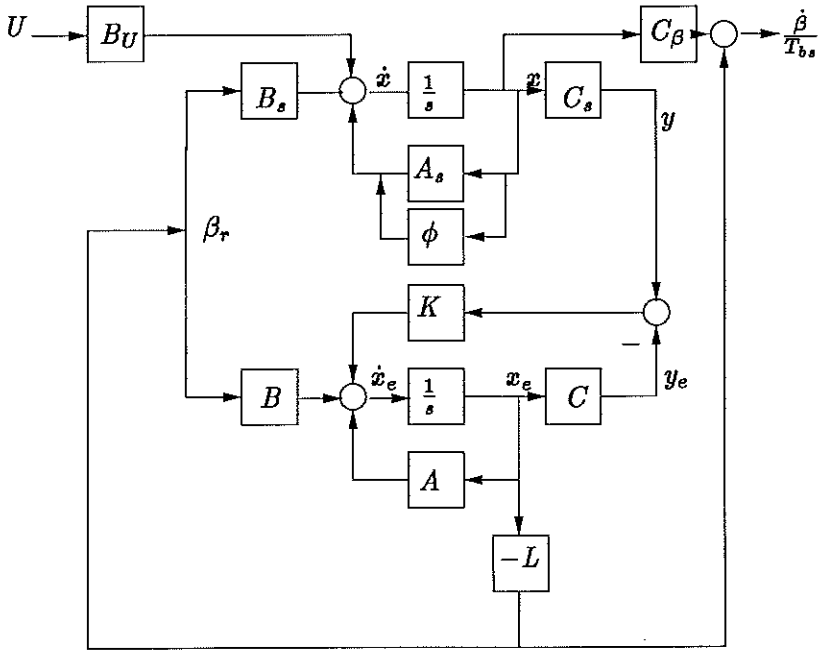

Figure 5.2 State Space model of system with observer and feed back

The state space equations can the be found directly from Figure 5.2 and the system can be completely restated with the equations:

$$\begin{aligned} \dot{x} &= A_s x - B_s L x_e + B_U U + \beta_\phi^T w \\ \dot{x}_e &= KC_s x + (A - KC - BL)x_e \\ v &= \alpha_\phi x \end{aligned} \tag{5.3}$$

where v,w are connected through

$$w = \phi(t)v \tag{5.4}$$

as seen in Figure 5.1. This block diagram looks rather confusing and messy, and it is made clearer by lumping together the different parameters in one matrix.

The model then can be visualized in a general framework for robust performance analysis (see Figure 5.3). For this type of model the machinery of robust

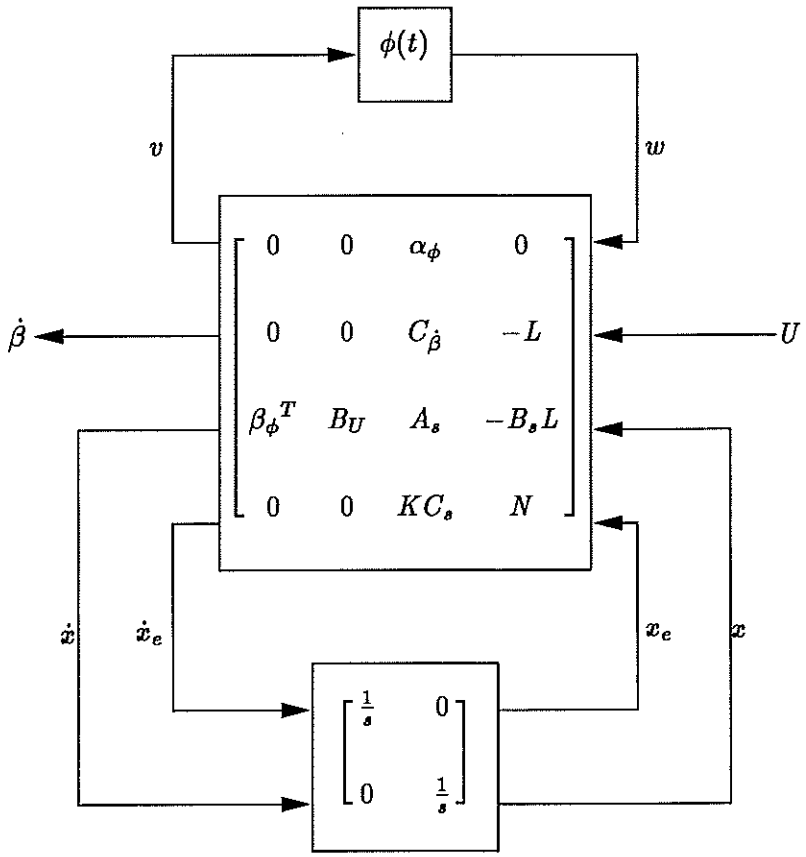

Figure 5.3 The System written in a General Framework for Robust Performance Analysis. Notice that $N = (A - KC - BL)$

analysis [Zhou [11]] can be utilized to move between different input, output variables and the "final destination" — the representation of Figure 5.1.

$$\begin{aligned} M(s) &= \begin{bmatrix} \alpha_\phi & 0 \\ C_{\dot{\beta}} & -L \end{bmatrix} \left(Is - \begin{bmatrix} A_s & -B_s L \\ KC_s & (A - KC - BL) \end{bmatrix} \right)^{-1} \begin{bmatrix} \beta_\phi{}^T & B_W \\ 0 & 0 \end{bmatrix} \\ &= \widetilde{C}(Is - \widetilde{A})^{-1}\widetilde{B} \end{aligned} \tag{5.5}$$

When the system is represented in the state-space with $\widetilde{A}$, $\widetilde{B}$, $\widetilde{C}$ and $\widetilde{D}$, it can be studied numerically in MATLAB's μ- and LMI-toolbox. For example, Equation 5.5 is calculated numerically in MATLAB. Thus, the formulation of Figure 5.1 can be studied.

Let $\phi(t)$ be given, as before, to be a time-varying uncertainty limited by a sector $\phi(t) \in [-1, 1]$ and

$$M(s) = \begin{bmatrix} M_{11}(s) & M_{12}(s) \\ M_{21}(s) & M_{22}(s) \end{bmatrix} \in RH_\infty \tag{5.6}$$

then the robust stability is evaluated in the loop of M_{11} as done in Chapter 3. Thus, $(I - M_{11}\phi)^{-1} \in RH_\infty$ for all $\phi(t) \in [-1, 1]$ for the system to be stable.

Robustness Performance

When analyzing the robustness we have to choose some limits on the uncertainty. From last chapter it is already shown that the system is stable for K_β varying in a ball of radius one around its operating point. For the robustness analysis this sector needs to be reduced, and a natural sector seem to be $K_\beta = 2 \pm 0.5$. The model (see Figure 5.1) is therefore scaled such that $\phi \in [-1, 1]$ correspond to this sector of K_β. The system is then studied through traditional as well as more modern techniques. First, the Nyquist curve is plotted for the elements of $M(s)$ to get some insight (see Figure 5.4). As ex-

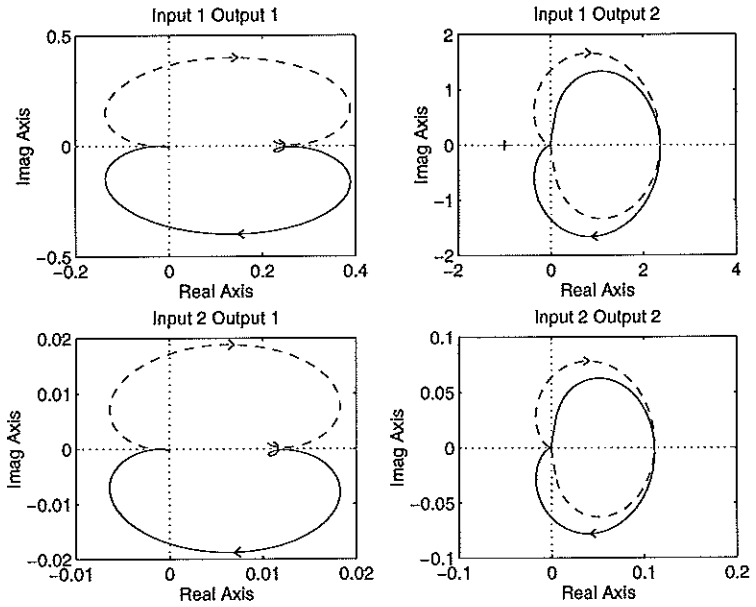

Figure 5.4 Nyquist plot of the elements of $M(s)$.

pected, the Nyquist contour of $M_{11}(S)$ is enclosed by the circle corresponding to $\phi \in [-1, 1]$ thus the system is stable. We can further notice that for the nominal plant (i.e. $\phi(t) = 0$) the transfer-function from u to $\dot{\beta}$ is given by $M_{22}(s)$ and the maximum amplitude can then be found to be 0.11 (rad/s)/(m/s) occurring at a frequency of approximately 4 (rad)/(s) (see Figure 5.4).

The upper limit of the gain (γ) from (u) to ($\dot{\beta}$) is found from the following S-procedure argument (see Figure 5.1).

Our assumption on $\phi(t)$ will be that

$$|\phi(t)| < 1 \quad \text{for all} \quad t. \tag{5.7}$$

Hence,

$$\int |w|^2 d\omega \leq \int |v|^2 d\omega \tag{5.8}$$

where $w(t) = \phi(t)v(t)$ (see Figure 5.1). From this assumption, we will compute a $\gamma \geq 0$ such that

$$\int |\dot{\beta}|^2 d\omega \leq \gamma^2 \int |U|^2 d\omega \tag{5.9}$$

for all $\dot{\beta}$, U satisfying the system equations. Obviously the implication from (5.8) to (5.9) holds if there exists an $x > 0$ such that

$$x||v||^2 - x||w||^2 + ||\dot{\beta}||^2 - \gamma^2||U||^2 \leq 0. \tag{5.10}$$

By noting that the system equations can be written as

$$\begin{aligned} \begin{bmatrix} v \\ w \end{bmatrix} &= \begin{bmatrix} M_{11} & M_{12} \\ 1 & 0 \end{bmatrix} \begin{bmatrix} w \\ U \end{bmatrix} \\ \begin{bmatrix} \dot{\beta} \\ U \end{bmatrix} &= \begin{bmatrix} M_{21} & M_{22} \\ 0 & 1 \end{bmatrix} \begin{bmatrix} w \\ U \end{bmatrix} \end{aligned} \tag{5.11}$$

the inequality (5.10) follows from the matrix inequality

$$\begin{aligned} &\begin{bmatrix} M_{11} & M_{12} \\ 1 & 0 \end{bmatrix}^* \begin{bmatrix} x & 0 \\ 0 & -x \end{bmatrix} \begin{bmatrix} M_{11} & M_{12} \\ 1 & 0 \end{bmatrix} + \\ &\begin{bmatrix} M_{21} & M_{22} \\ 0 & 1 \end{bmatrix}^* \begin{bmatrix} 1 & 0 \\ 0 & -\gamma^2 \end{bmatrix} \begin{bmatrix} M_{21} & M_{22} \\ 0 & 1 \end{bmatrix} \leq 0. \end{aligned} \tag{5.12}$$

by multiplication from the right and left by $[w \quad U]^T$.

This equation can then be solved numerically in MATLAB's LMI-toolbox to find the minimal value of γ^2 for all $x \in R^+$ such that the equality is true.

REMARK 5.1
It is useful to rewrite the inequality 5.12 to:

$$\begin{bmatrix} M(j\omega) \\ I \end{bmatrix}^* \begin{bmatrix} x & 0 & 0 & 0 \\ 0 & 1 & 0 & 0 \\ 0 & 0 & -x & 0 \\ 0 & 0 & 0 & -\gamma^2 \end{bmatrix} \begin{bmatrix} M(j\omega) \\ I \end{bmatrix} \leq 0 \quad \forall\omega \tag{5.13}$$

which can be transformed to:

$$\begin{bmatrix} (j\omega - A)^{-1}B \\ I \end{bmatrix}^* C^T(H_0 + xH_1 + \gamma^2 H_3)C \begin{bmatrix} (j\omega - A)^{-1}B \\ I \end{bmatrix} \leq 0. \tag{5.14}$$

By applying the Kalman- Yakubovich- Popov Lemma, as stated by Willems [[10]], the inequality above is equivalent to the existence of a symmetric $P = P^T$ such that:

$$C^T(H_0 + xH_1 + \gamma^2 H_3)C + \begin{bmatrix} A^TP + PA & PB \\ B^TP & 0 \end{bmatrix} \leq 0. \tag{5.15}$$

This problem is of a form which can easily be solved numerically utilizing modern optimization algorithms in MATLAB's LMI-toolbox. □

Notice that the inequality (5.10) does not take into account the periodicity of the uncertainty.

When minimizing γ for the robust performance of the input output pair U to $\dot{\beta}$, the solution is $\gamma = 0.19$ (rad/s)/(m/s) which gives us the upper limit of the amplification. Thus, we can give the interval $\gamma \in [0.11, 0.19]$ within

Table 5.1 Change in limits of γ as a function of K_β

K_β		γ	
		min	max
0.75	± 0.25	0.15	0.29
1	± 0.33	0.13	0.29
1.5	± 0.5	0.12	0.27
2	± 0.67	0.11	0.19
2.5	± 0.83	0.12	0.30
3.0	± 1.0	0.13	0.42

which γ will vary. Recall that the lower bound of γ is found by analyzing the nominal-plant with no uncertainty. Moreover, the lower bound is found by looking at the maximum amplitude of $M_{22}(s)$ for all s.

How much pitch movement can we tolerate? Engineering judgment must be used to answer this question, but from the dynamics of the wind it can be assumed that the tower-blockage will be a greater problem than the wind variation by itself.

Robust Performance under Tower Blockage

When analyzing for the perturbation of the tower blockage, the same circles as in Chapter 4 is studied (see Figure 5.5). The interval of γ is then determined

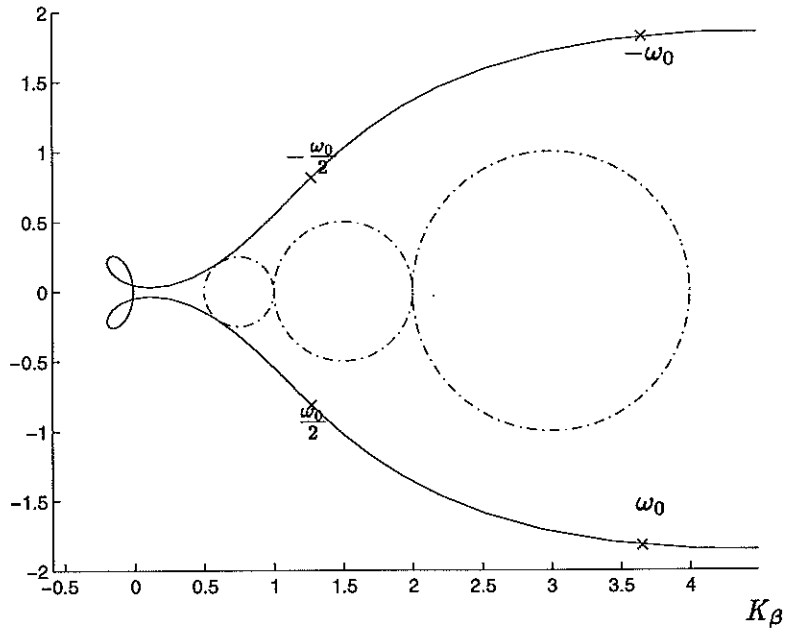

Figure 5.5 Inverse Circle Criterion with Circles Corresponding to Tower Blockage

for each of the circles and the result is presented in Table 5.1.

Thus, since the tower blockage occurs with a frequency of 5.2 rad/s, γ in the range of 0.4 (rad/s)/(m/s) will force the servo to oscillate very much. In fact $\gamma \in [0.11, 0.42]$ will force the system to oscillate at the frequency $2P$ with amplitudes of $0 - 6°$.

The amplitude interval due to the tower-blockage is a function of the nominal K_β (see Figure 5.6. Figure 5.6 shows that the robust performance is best

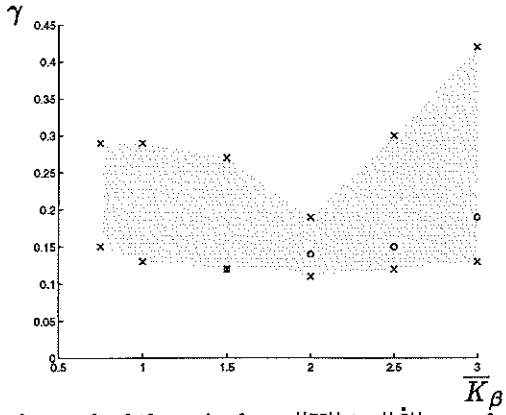

Figure 5.6 The interval of the gain from $||U||$ to $||\dot{\beta}||$ as a function of $\overline{K}_\beta$. The o's correspond to the simulated values using the sophisticated nonlinear from Sven Erik Mattsson.

around the nominal value $K_\beta = 2$ which also is the value the controller is designed for.

When evaluating these values of the gain from $||U||$ to $||\dot{\beta}||$, it is found to be to large; thus, it creates unacceptable β movement at the frequency of $2P$.

Notice (Figure 5.6) that the upper limit of γ drops to its minimum at the operating point which the controller is designed for, but increases rapidly as the $|\Delta\phi|_{max}$ (and K_β) increases.

New Design, More Robust for the Tower Blockage

Since so much of the noise is frequency dependent with the frequency $2P$, a penalty on $\dot{\beta}$ for this frequency is needed. This is done by introducing an inverse notch-filter (see Figure 5.7) on of frequency $2P$ to the $\dot{\beta}$. This filter is implemented in the state-space model, and the feedback is designed with weight on $\dot{\beta}$ by LQG.

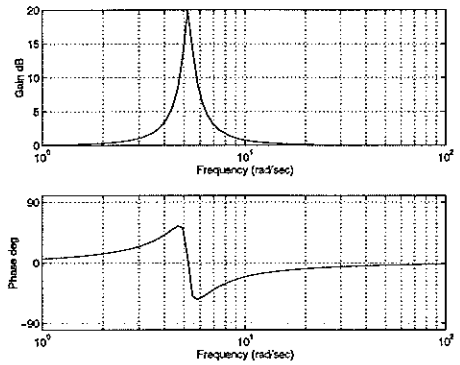

Figure 5.7 Inverse Notch-filter for Penal-Ising the 2P Frequency

We then follow the same analysis step for this new model and determine the gain (γ) from $||U||$ to $||\dot{\beta}||$ for the tower-blockage perturbation. The new intervals for γ looks as follows in Table 5.2.

The gain has decreased with a factor of more than 8 for operating points up to $K_\beta = 2.5$, and the oscillations is not longer a problem. For comparison the gain interval is plotted as a function of the operating point. From Figure 5.8

Table 5.2 Change in limits of γ as a function of K_β

K_β		γ	
		min	max
0.75	± 0.25	0.0209	0.0361
1	± 0.33	0.0195	0.0387
1.5	± 0.5	0.0176	0.0412
2	± 0.67	0.0176	0.0469
2.5	± 0.83	0.0200	0.0670
3.0	± 1.0	0.0226	0.203

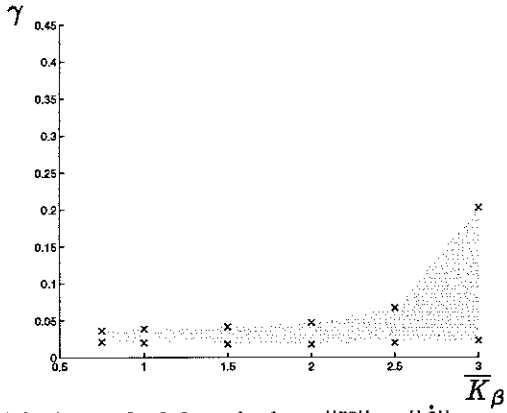

Figure 5.8 The interval of the gain from $||U||$ to $||\dot{\beta}||$ as a function of $\overline{K}_\beta$

we can see that the inverted notch-filter has less effect when $|\Delta\phi|_{max}$ is high. Thus, the new design is not improved by more than a factor 2 for wind-speeds in the range of $27m/s$.

5.2 Robust Performance of the Power Output

In our design, the goal for the electrical power (P_E) is to keep it constant by controlling the pitch angle. We want to analyze the effect variations in the wind has on P_E. Ideally, the wind changes would not be transfered out to the electrical net, but in reality this is hard to hinder.

The next variable pair we analyze is, therefor, the change in wind-speed (U) to the change in electrical power output (P_E). The wind power-plant is allowed to have a variation of about 40% in P_E.

Since earlier analysis have suggested that the the tower-blockage is the main cause of poor-performance, the pair is evaluated for the tower-blockage, and the same sectors are used as before.

First the evaluation is made for the wind-dynamics of a low-pass filter (Equation 2.5). This evaluation gives gains as seen in Table 5.3. Notice that the output is represented as % of $P_{E0} = 3MW$.

When introducing the notch-filter the estimated bounds for the performance changes slightly for K_β's up to 2.5, but dramatically for higher values of K_β. This can be seen in connection to the large perturbation at this nominal values (for example at $\overline{K}_\beta = 3$ the uncertainty is $\phi(t) \in [-1, 1]$).

Table 5.3 Change in limits of γ as a function of K_β

K_β		γ	
		min	max
0.75	$\pm.25$	30.37	58.51
1.0	$\pm.33$	24.55	52.21
1.5	±0.5	16.22	39.73
2.0	$\pm.67$	12.05	30.57
2.5	$\pm.83$	9.33	25.13
3.0	±1.0	7.85	26.90

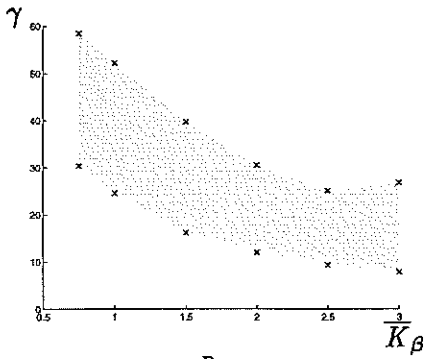

Figure 5.9 The gain from $||U||$ to $||\frac{P_E}{P_{E0}}100||$ varying with nominal value of $\overline{K}_\beta$

In Table 5.4 it can be seen that the robustness is slightly worst for the system after the new design.

With the information we have gained from this analysis it was tempting to designing a tighter control on the power, since stability of the system not is seen as being a major problem. This was done, but when the P_E control was tightened, the gain for $\dot{\beta}$ immediately gave unacceptable values.

Table 5.4 Change in limits of γ as a function of K_β

K_β		γ	
		min	max
0.75	$\pm.25$	30.11	58.23
1.0	$\pm.33$	27.72	55.46]
1.5	±0.5	19.95	47.70
2.0	$\pm.67$	15.14	41.85
2.5	$\pm.83$	12.45	44.51
3.0	±1.0	12.88	118.20

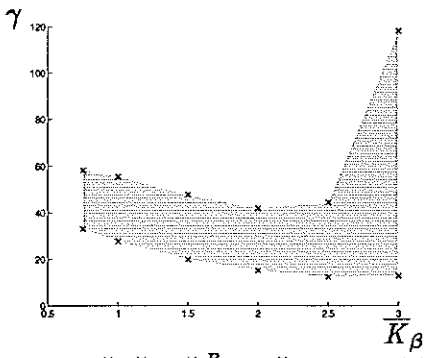

Figure 5.10 The gain from $||U||$ to $||\frac{P_E}{3E6}100||$ varying with nominal value of $\overline{K}_\beta$

5.3 Conclusion of Performance Analysis

The robust performance analysis carried out in this chapter gives a good measure of the system behavior under the influence of uncertain parameters. The evaluation suggests that the tower-blockage is one of the major problems for the performance, and this perturbation is, therefore, studied in detail.

From the analysis it was found that $\dot{\beta}$ changed to much for wind variations. To reduce this problem for the tower-blockage a heavier wait was given to the frequency of $2P$ (the frequency of the tower blockage perturbation). This was done by introducing an inverted notch filter on $\dot{\beta}$. The new design gives a better behavior for $\dot{\beta}$, but the effect of the new design is not very convincing for large variation in the uncertainty (i.e. $|\phi(t)| \in [-1, 1]$ see Figure 5.8).

When analyzing the performance of the electrical power (P_E), the control is found to be rather loose. Wind variations have a large impact on the power output. The reason for this is that the control problem is difficult, and the different control aspects have been weight against each other. Priority has been given to the size of $\dot{\beta}$ in the cost function and P_E has a looser control.

In the chapter some of the analysis have been confirmed through simulations in Simnon — using the complex model of the wind power plant [Mattsson [6]] (with minor modifications). The power plant is constructed to produce rated power ($3MW$) at a wind speed of 14.2 m/s [Mattsson [6] p.75], and the simulations are therefore verifying my estimations for wind speeds greater than this (corresponding to $K_\beta \geq 1.5$).

As a final remark, it is worth noting that when analyzing the tower blockage, the analysis is also too conservative not taking count of the periodicity of the perturbation. This could be changed by using a frequency varying x when optimizing the linear matrix inequality.

6. Conclusion

The power plant is found to be stable for all perturbations examined. This means that the linearization used for controller design was not critical for the stability. It should however be noticed that that tightening the control more does not seem to give the effect desired. Even though a tighter control still will be stable, the performance is not improved. The reason for this is that the performance for the servo speed and the power output are dependent on each other in some sense, and penalising one more leave less for the other.

In the design the pitch movement $\dot{\beta}$ has been given priority, but this leaves us with a very loose control on power output P_E. It was tried to tighten this but it imposed a loose control on $\dot{\beta}$. Thus to get a better performance on both the variables we need to use more sophisticated design than a simple LQG. One idea would be to further explore the gain scheduling control proposed by Mattsson [6].

When the control was designed for the power plant, the theory for analysing the effects of uncertainty was limited. Simulations were used to evaluate robustness, and traditional techniques as amplitude and phase margins used to design the plant. The techniques used in this thesis gives a more direct evaluation of the uncertainty. Instead of using engineering judgement to decide when we have enough phase margin this method enable us to see more direct how the uncertainty affects the stability and performance.

The stability criterion by Willems enables us to show stability in a less conservative way than the Circle criterion. Since the wind power plant itself behaves periodically, many of its parametric uncertainties will behave periodic. Some of them with the same frequency as the turbine and other with different frequency (recall the up stepping gear).

7. Acknowledgments

I want to thank both my supervisors Sven Erik Mattson and Anders Rantzer. It has been a true pleasure doing my Master thesis with you both.

Anders and Sven Erik have both been very helpful and supporting, giving me a great opportunity to get a taste of their fields of research. Thanks for putting together a very interesting project which were based on a practical problem that were theoretically challenging. This have given me new knowledge and a hunger for digging deeper into the material.

My stay in Lund have been a great pleasure, and I am glad I got the opportunity to work in this friendly department. I would like to express my sincere thanks to : Professors, PhD students, technical staff, secretaries, visiting scientists and master students.

I also want to thank Professor Professor Karl-Johan Åström and Björn Wittenmark for letting me do my thesis at Lund Institute of Technology.

Furthermore I would like to thank The Norwegian Business Foundation and the Norwegian State Educational Loan Found for sponsoring my studies in University of California, Santa Barbara and Imperial College, University of London.

Finally, I want to thank the people I share office with Cesar Mendoza and Sabina Brufani. It has been great fun, and thanks for the burritos and spaghetti.

8. Appendix: numerical values of parameters

Operating point values for State-space model 2.6:

$$
\begin{aligned}
\dot{x} &= Ax + B\beta_r + B_U U \\
y &= Cx \\
x &= \begin{bmatrix} \Delta\beta \\ \frac{\Delta U}{100} \\ \Delta\dot{\gamma} \\ \Delta\gamma \end{bmatrix}, \qquad A = \begin{bmatrix} -2.5 & 0 & 0 & 0 \\ 0 & -0.05 & 0 & 0 \\ 2.0 & 4.7 & -0.47 & -1.5 \\ 0 & 0 & 1 & 0 \end{bmatrix} \\
B &= \begin{bmatrix} 2.5 \\ 0 \\ 0 \\ 0 \end{bmatrix}, \qquad B_U = \begin{bmatrix} 0 \\ 0.0057 \\ 0 \\ 0 \end{bmatrix} \\
y &= \begin{bmatrix} P_E \\ \dot{\psi} \end{bmatrix}, \qquad C = \begin{bmatrix} 0 & 0 & 7.85 & 20.16 \\ 0 & 0 & 1 & 0 \end{bmatrix}
\end{aligned}
\tag{8.1}
$$

Equation 4.6

$$
\begin{aligned}
\dot{x} &= Ax + r \\
\dot{x_e} &= Ax_e + B\beta + K(Cx - Cx_e) \\
\beta_r &= -0.379\beta - [3.26 \quad 1.21 \quad 0.954]\, x_e \\
\dot{\beta} &= -0.4\beta + T_{bs}\beta_r
\end{aligned}
\tag{8.2}
$$

9. Bibliography

[1] J. Allwright. Course notes in: Non-linear control. Imperial College, University of London, 1995.

[2] I. Jaimouka. Course notes in: Multivariable control. Imperial College, University of London, 1995.

[3] Ulf Jonsson and Anders Rantzer. Systems with uncertain parameters - time-variations with bounded derivatives. Lund Institute of Technology, 1996.

[4] Hassan K. Khalil. *Nonlinear Systems.* Macmillan, 1992.

[5] P. V. Kokotovic, Hassan K. Khalil, and Jhon O'Reilly. *Singular Perturbation in Control: Analysis and Design.* Academic Press, 1984.

[6] Sven Erik Mattsson. *Modelling and Control of Large Horizontal Axis Wind Power Plants.* PhD thesis, 1984.

[7] Alexander Megretski and Anders Rantzer. System analysis via integral quadratic constraints. Technical report, April 1995.

[8] Fernando Paganini. *Set and Constraints in the Analysis of Uncertain Systems.* PhD thesis, 1996.

[9] Jean-Jacques E. Slotine and Weiping Li. *Applied Nonlinear Control.* Prentence Hall, 1991.

[10] Jan C. Willems. On the stability of the null solution of linear diferential equations with periodic coefficients. *IEEE Transactions on Automatic Control*, 13(1):65–72, 1968.

[11] Kermin Zhou, John C. Doyle, and Keith Glover. *Robust and Optimal Control.* Prentice Hall, 1995.